1

Introduction

1.1 Infrared Radiation

1.1.1 Technical Applications

Infrared (IR) radiation is an electromagnetic radiation in the wavelength range between visible radiation (often abbreviated as VIS; $\lambda = 380$–$780\,\text{nm}$) and microwave radiation ($\lambda = 1\,\text{mm}$–$1\,\text{m}$). IR radiation has some physical characteristics that make them particularly suitable for a number of technical applications:

- Each body emits electromagnetic radiation (see Section 2.3). The radiation depends on the wavelength and is determined by the body's temperature. Thus the measured radiation can be used to measure the body's temperature. This characteristic is used for contactless temperature measurement (pyrometry).
- For high temperatures of several 1000 K, the maximum falls within the visible range; the human eye has adapted its highest sensitivity to $\lambda \approx 550\,\text{nm}$, corresponding to the surface temperature of the sun (approximately 6000 K). Opposed to this, at ambient temperature the irradiation of bodies has an infrared maximum of about $10\,\mu\text{m}$ (see Figure 3.2.1). This can be used to detect the presence and motion of people (motion detectors, security systems) or to record entire scenes with IR cameras – similar to video cameras. The latter has the advantage that parts of the IR spectrum allow the propagation of radiation even in darkness or under foggy conditions – the basis for night vision devices and driver assist systems.
- IR cameras can also be used for recording thermal images showing the thermal isolation of buildings, temperature distribution of combustion processes or temperature-dependent processes. Today, commercial thermal cameras have an image resolution similar to that of high-resolution TV.
- Electromagnetic radiation can induce oscillations in the atoms of molecules. In that case distance and angle of the bonds between atoms, for instance, change periodically. Each bond has a specific resonance frequency at which the radiation is almost completely absorbed.

Thermal Infrared Sensors: Theory, Optimisation and Practice Helmut Budzier and Gerald Gerlach

As radiation frequency v and wavelength λ are coupled via propagation velocity c.

$$\lambda = \frac{c}{v} \tag{1.1.1}$$

Chemical compounds absorb radiation at characteristic wavelengths. Many of these absorption wavelengths fall within the IR range. IR radiation with a specific wavelength can thus be used to determine the presence and concentration of specific substances, which can be applied for the gas analysis. If we record complete reflexion and transmission spectres of irradiated samples, the position of the absorption bands can be used to draw conclusions about their chemical composition (IR spectrometry).

Looking at the mentioned characteristics and the corresponding technical applications, the typical structure of infrared measuring systems becomes apparent (Table 1.1.1). The

Table 1.1.1 Typical structure of infrared sensors and measuring systems

Application	Radiation source	Propagation path	Imaging system	Sensor/Sensor array
	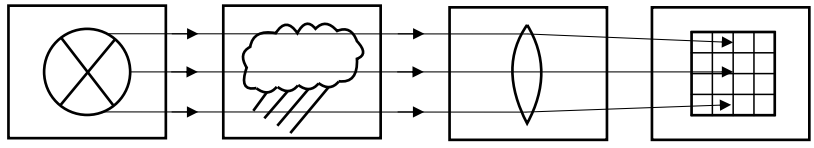			
Pyrometer	Measuring object (with background)	Atmosphere, optical fibre	Lens, filter	Single- or multi-element sensor (mainly thermal or pyroelectric)
Thermal imaging device	Measuring object with background/ Thermal imaging scene	Atmosphere	Lens, filter	Sensor array (FPA Focal Plane Array, mainly bolometer)
Passive motion detector	Measuring object with background	Atmosphere	Fresnell-optics	Two-element sensor (mainly pyroelectric)
Gas sensor	Thermal (e.g. glow emitter, hotplate) or non-thermal emitter (LED, Laser)	Gas cell or atmosphere with measuring gas	Lens, filter	Multi-element sensors (mainly thermal or pyroelectric)
Spectrometer	Thermal (e.g. glow emitter) or tunable, non-thermal emitter (LED, Laser)	Chemical compound	Grating, mirror	Single-element or array sensors (mainly thermal or pyroelectric)
Relevant book chapters	Chapter 2	Section 2.1	Chapter 3, Section 5.5	Section 2.1, Chapter 4 to 6

measuring object can be the IR radiation source itself (pyrometry, thermal imaging, motion detectors) or affect the transmission of the propagation path (gas analysis, spectroscopy/ spectrometry).

The structure of this book follows the measuring chain presented in Table 1.1.1, which means that Chapter 2 will discuss the origin and propagation of electromagnetic radiation. The radiation sources will be limited to thermal emitters as they themselves constitute the measuring object in pyrometers, thermal imaging devices as well as motion detectors and are preferably used in gas analysis and spectrometry.

Section 2.1 discusses the effect that the propagation of electromagnetic radiation occurring on the propagation path has, particularly on the detection of chemical species.

Chapter 3 presents the photometric basics including mapping the radiation source area to the area of the sensor or sensor array. As in most applications the IR radiation is emitted from an emitter's surface into space; we will put particular emphasis on the solid angle relations between radiation source and sensor. Due to the huge variety, classical optical elements such as lenses, gratings or filters will not be included, as this is not a book on optics. An exception will be made in Section 5.5, which will introduce the optical parameters that are important for sensor arrays.

Chapter 5 describes the characteristics of infrared optical sensors and sensor arrays. As the minimum detectable radiant fluxes or temperature differences, respectively, are determined by physically unavoidable noise processes, Chapter 4 will introduce the basics and the most important noise sources for IR sensors.

Chapter 6 describes the structure and characteristics of important thermal infrared sensors. We limit the discussion to thermal IR sensors as they do not have to be cooled and therefore can be miniaturised and are comparatively inexpensive (thermal imaging cameras with HDTV resolution are currently already available for only several thousand to tens of thousands Euro). They have come to clearly dominate the civil applications' market.

Chapter 7 finally presents an overview of the basics presented in the previous chapters for the applications included in Table 1.1.1.

1.1.2 Classification of Infrared Radiation

Infrared radiation is a high-frequency electromagnetic radiation. For the propagation in linear-optical components (vacuum, air, glass, silicon), frequency v remains constant, whereas wavelength λ can change depending on wave propagation (light) velocity c in different media:

$$\lambda = \frac{c}{v} = \frac{c_0}{n\,v} \tag{1.1.2}$$

where c_0 is the speed of light in vacuum and n the refractive index. In spectroscopy, wave number σ is often used as the reciprocal of the wavelength:

$$\sigma = \frac{1}{\lambda} \tag{1.1.3}$$

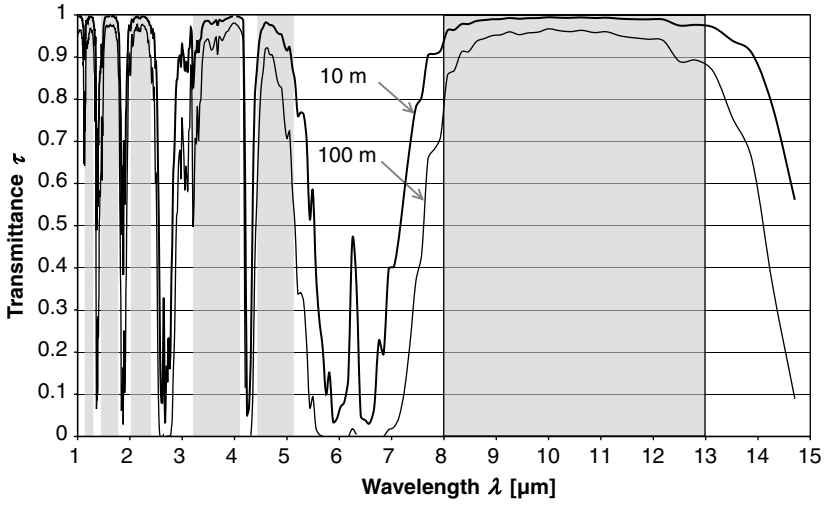

Figure 1.1.1 Typical transmission in atmosphere during summer in Central Europe. Parameter: Length of propagation path

Wavelength ranges can be classified according to several criteria. In the following, we will present the classification that is commonly used in infrared measuring technology and that results from transmission τ of the atmosphere due to the absorption of water vapour (H_2O) and carbon dioxide (CO_2) in the air (Figure 1.1.1). For all applications where the atmosphere constitutes the transmission path, only selected wavelength ranges – atmospheric windows – can be used (areas shaded in grey in Figure 1.1.1; Table 1.1.2).

Table 1.1.2 Atmospheric windows

Atmospheric window	Infrared region	Wavelength range in µm	Temperature range of max. exitance acc. to Equation. 2.3.6 in K	Remarks
I	Near infrared (NIR)	1.2–1.3	2415–2229	Emission of hot bodies (>1000 °C)
		1.5–1.7	1932–1705	
		2.1–2.4	1380–1208	
II	Mid infrared (MIR)	3.2–4.1	906–707	Emission of hot bodies (>300 °C)
		4.4–5.2	659–557	Absorption of CO_2 and other gasses
III	Far infrared (FIR)	8–13	362–223	Emission of bodies at room temperature

Table 1.1.3 Classification of infrared radiation

Range		Wavelength λ (μm)	Wave number σ (cm^{-1})	Frequency (v)[a] (THz)	Photon energy E^b (eV)
VIS		0.38–0.78	26 316–12 821	789–384 THz	3.27–1.59
IR	NIR	0.78–3	12 821–3333	384–100 THz	1.59–0.41
	MIR	3–6	3333–1667	100–50 THz	0.41–0.21
	FIR	6–40	1667–250	50–7.5 THz	0.21–0.03
	UFIR	40–1000	250–10	7.5 THz–300 GHz	$0.03–1.2 \times 10^{-3}$

[a] $v/\mathrm{Hz} = \dfrac{299.8 \times 10^{12}}{\lambda/\mu\mathrm{m}}$

[b] $E/\mathrm{eV} = \dfrac{1.241}{\lambda/\mu\mathrm{m}}$

In the optimal case, the maximum of the radiation source's specific irradiation lies exactly in the selected range (WIEN's displacement law; Equation. 2.3.6).

In correspondence to the atmospheric windows in Table 1.1.2, the infrared radiation range can be divided into near- (NIR), mid- (MIR), far- (FIR) and ultrafar- (UFIR) infrared (Table 1.1.3).

Here, monochromatic radiation is radiation of a single frequency or wavelength, respectively. Mostly though, radiation consists of many wavelengths (or frequencies) and we have to look at the corresponding spectral ranges.

1.2 Historical Development

Table 1.2.1 summarises the historical development of infrared measuring technology. The starting point was the discovery by Sir WILHELM HERSCHEL in 1800, that for the spectral decomposition of light the largest temperature rise occurred in the invisible spectral range beyond the red (*Philosophical Transactions of the Royal Society of London*, **XIII**, April 24, 1800, page 272, quoted in Caniou [1]). Later on he showed that also invisible radiation from other hot sources such as fire, candlelight or a red-hot oven emit invisible radiation that behaves according to the laws of optics regarding reflexion and diffraction. Initially this radiation was called 'ultra-red', but later the term 'infrared' was introduced.

Further development stages focused on the proof that thermal radiation and electromagnetic waves are of the same nature (first half of the nineteenth century). MAX PLANCK'S works formulating the light-quantum hypothesis and the derivation of PLANCK'S radiation laws in 1900 as well as the formulation of the law of the external photoeffect in 1905 and the assumption of stimulated emission by ALBERT EINSTEIN constituted the decisive fundamentals for the quantum nature of the interaction of electromagnetic radiation and solid-state bodies. Thus, the essential physical bases for the technical utilisation of infrared radiation in IR measuring technology were established.

Table 1.2.1 Milestones in the development of infrared measuring technology (according to [1] and [2])

Year	Event
1800	Discovery of the existence of thermal radiation in the invisible beyond the red by W. Herschel
1822	Discovery of the thermoelectric effects using an antimony–copper pair by T. J. Seebeck
1830	Thermal element for thermal radiation measurement by L. Nobili
1833	Thermopile consisting of 10 in-line Sb-Bi thermal pairs by L. Nobili and M. Melloni
1834	Discovery of the Peltier effect on a current-fed pair of two different conductors by J. C. Peltier
1835	Formulation of the hypothesis that light and electromagnetic radiation are of the same nature by A. M. Ampère
1839	Solar absorption spectrum of the atmosphere and the role of water vapour by M. Melloni
1840	Discovery of the three atmospheric windows by J. Herschel (son of W. Herschel)
1857	Harmonisation of the three thermoelectric effects (Seebeck, Peltier, Thomson) by W. Thomson (Lord Kelvin)
1859	Relationship between absorption and emission by G. Kirchhoff
1864	Theory of electromagnetic radiation by J. C. Maxwell
1879	Empirical relationship between radiation intensity and temperature of a blackbody by J. Stefan
1880	Study of absorption characteristics of the atmosphere through a Pt Bolometer resistance by S. P. Langley
1883	Study of transmission characteristics of IR-transparent materials by M. Melloni
1884	Thermodynamic derivation of the Stefan law by L. Boltzmann
1894, 1900	Derivation of the wavelength relation of blackbody radiation by J. W. Rayeigh and W. Wien
1903	Temperature measurements of stars and planets using IR radiometry and spectrometry by W. W. Coblentz
1914	Application of bolometers for the remote exploration of people and aircrafts
1930	IR direction finders based on PbS quantum detectors in the wavelength range 1.5–3.0 µm for military applications (Gudden, Görlich and Kutscher), increased range in World War II to 30 km for ships and 7 km for tanks (3–5 µm)
1934	First IR image converter
1939	Development of the first IR display unit in the US (Sniperscope, Snooperscope)
1947	Pneumatically acting, high-detectivity radiation detector by M.J.E. Golay
1954	First imaging cameras based on thermopiles (exposure time of 20 min per image) and on bolometers (4 min)
1955	Mass production start of IR seeker heads for IR guided rockets in the US (PbS and PbTe detectors, later Sb detectors for Sidewinder rockets)
1965	Mass production start of IR cameras for civil applications in Sweden (single-element sensors with optomechanical scanner: AGA Thermografiesystem 660)
1968	Production start of IR sensor arrays (monolithic Si-arrays: R.A. Soref 1968; IR-CCD: 1970; Schottky diode arrays: F.D. Shepherd and A.C. Yang 1973; IR-CMOS: 1980; SPRITE: T. Eliott 1981)
1995	Production start of IR cameras with uncooled FPAs (Focal Plane Arrays; microbolometer-based and pyroelectric)

1.3 Advantages of Infrared Measuring Technology

Infrared radiation has a number of advantages that make it very useful for contactless temperature measuring, in particular, and infrared measuring technology, in general.

- It is contactless and therefore (almost) reactionless. As the radiation energy exchange also takes place from the sensor to the radiation source, it would not be correct to talk about a complete absence of feedback. However, this feedback on the radiation source can – in general – be neglected (see Section 6.1 and Figure 6.1.3).
- It spatially separates radiation source and detector, which means that also very hot or otherwise difficult-to-access objects can be measured.
- It allows fast measurements as it propagates at the speed of light and the characteristic time constants of measuring process can be kept very small, due to miniaturisation (see Example 6.2.2 and Figure 6.2.6, for instance).
- It allows measuring of the temperature of a solid-state body surface and not that of the surrounding atmosphere.

These characteristics enable the contactless examination or temperature measurement of the following objects and measuring points:

- Fast-moving objects. Contactless measuring avoids interferences caused by contacting temperature sensors, rotation or friction.
- Current-carrying objects. Current-carrying components and devices pose a potential risk for both measuring equipment and operating staff. Contactless remote sensing can be used to avoid such risks.
- Small objects. The larger the temperature sensor is in relation to the object to be measured the more the temperature measured by the temperature sensor increases. Due to the adjustable imaging system (see Table 1.1.1) of IR measuring system, such interference can be largely avoided.
- Measuring at unaccessible measuring points. Many industrial measuring processes are carried out under very harsh conditions, for example at high temperatures that would destroy contacting temperature sensors. The IR-based contactless measuring technology provides technical solutions for such measuring tasks.
- Parallel measurements at several measuring points. In case of contact sensors, measuring processes with measurements at several points require complex solutions. Sensing measuring systems or image-based measuring procedures are a much more (cost-)efficient solution for such measuring tasks (quantitative thermograms or thermal imaging).

1.4 Comparison of Thermal and Photonic Infrared Sensors

In principle, we distinguish two kinds of infrared sensors (Figure 1.4.1):

- thermal sensors and
- photon or quantum sensors.

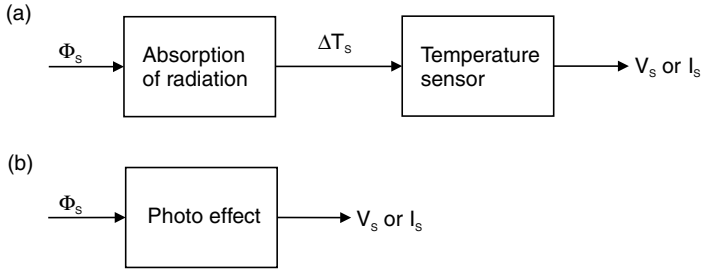

Figure 1.4.1 Active principle of (a) thermal and (b) photon or quantum radiation detectors, respectively

Thermal sensors are radiation detectors that, due to the absorption of IR radiation, experience a change in temperatures and convert it into an electric output signal (Figure 1.4.1a). They are therefore often called radiation temperature sensors. Looking at a sensor with current output I_S, without loss of generality, the following relation results for the current responsivity (index I):

$$R_I = \frac{\Delta I_S}{\Delta \Phi_S} \tag{1.4.1}$$

with change ΔI_S of the current sensors due to the change of radiant flux $\Delta\Phi_S$ (unit Watts) absorbed in the sensor (see Equation 5.1.2). For energetic reasons, a specific radiant flux causes a proportional temperature increase ΔT_S in the sensor and subsequently, a proportional output current ΔI_S. Theoretically, energy absorption and thus temperature dependency ΔT_S is independent of wavelength, which means that also R_I is unrelated to wavelength. In practice, radiation absorption shows a certain wavelength dependency, though.

Specific detectivity D^* shows the relation resulting from responsivity R_I and the effective value of noise currents $\tilde{i}_{Rn}$ that falsify the sensor output current; and it is therefore a measure of the signal-to-noise ratio (SNR). D^* is normalised to the root of sensor surface A_S:

$$D^* = \frac{\sqrt{A_S}}{\tilde{i}_{Rn}} R_i \tag{1.4.2}$$

Apart from the dynamics of the incident IR radiation, the result is a wavelength-independent effective value of the sensor output current and thus a wavelength-independent, specific detectivity D^* of thermal sensors:

$$D^* \neq D^*(\lambda) \tag{1.4.3}$$

It is only natural to observe that the wavelength-dependency of the absorption of sensor materials causes a wavelength-dependency of responsivity R_I or specific detectivity D^*, respectively, of thermal sensors.

As opposed to this, radiant flux Φ_S impinging on photon detectors causes a completely different wavelength-dependency.

The incident radiant flux (radiation power) Φ_S on the sensor corresponds to radiation energy dQ impinging on the sensor per time unit dt (for a detailed presentation, see Section 2.2):

$$\Delta\Phi_S = \frac{dQ}{dt} \tag{1.4.4}$$

Radiation energy Q is the sum of energy contributions $h \cdot v$ of N photons:

$$\Delta\Phi_S = \frac{dQ}{dt} = \frac{d(N \cdot h \cdot v)}{dt} = hv\frac{dN}{dt} \tag{1.4.5}$$

For quantum detectors, each photon on average contributes η electrons to the current conduction. η is the quantum efficiency. Sensor current ΔI_S thus becomes

$$\Delta I_S = \frac{d(\text{Charge})}{dt} = \frac{d(\eta Ne)}{dt} = \eta e\frac{dN}{dt} \tag{1.4.6}$$

It results from Equations 1.4.5 and 1.4.6 that current responsivity R_I of a quantum detector is (see Section 5.1):

$$R_I = \frac{\Delta I_S}{\Delta\Phi_S} = \frac{\eta e}{h\,v} = \frac{\eta e}{hc}\lambda \tag{1.4.7}$$

Thus, the responsivity of photon sensors increases with increasing wavelength. This can be illustrated if we look at the radiation of two different wavelengths λ_1 and $\lambda_2 = 2\lambda_1$:

$$Q = N_1 h\,v = N_1\frac{h\,c}{\lambda_1} = N_2\frac{h\,c}{\lambda_2} \tag{1.4.8}$$

If radiation energy Q is the same in both cases, radiation of wavelength λ_2 contains exactly twice as many photons

$$N_2 = N_1\frac{\lambda_2}{\lambda_1} = 2N_1 \tag{1.4.9}$$

because its photon energy $h \cdot v_2$ is only half as large as $h \cdot v_1$:

$$h \cdot v_2 = h\frac{c}{\lambda_2} = h\frac{c}{2\lambda_1} = \frac{1}{2}(h \cdot v_1) \tag{1.4.10}$$

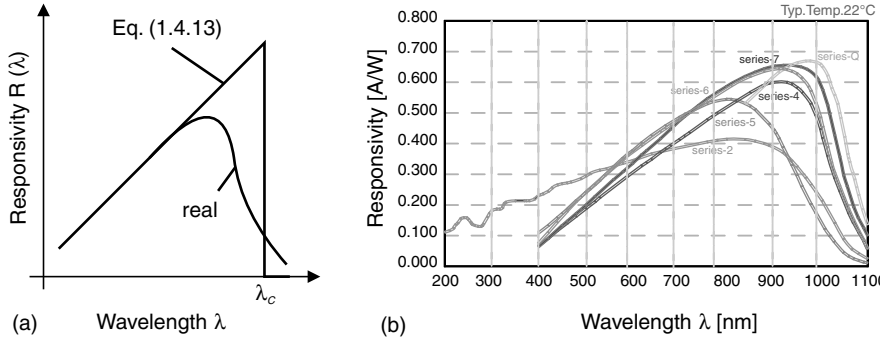

Figure 1.4.2 Wavelength-dependent responsivity of photon sensors. (a) schematic representation, (b) Si-pin-photo diodes (by courtesy of Silicon Sensor GmbH), the serial numbers characterise photo diodes with specifically optimised characteristics

Problems arise if wavelength λ is very large and thus the photon energy too small for the energy to be sufficient to transport the electrons from the valence band via energy gap E_G to the conduction band:

$$h \cdot v = \frac{hc}{\lambda} < E_G \tag{1.4.11}$$

or respectively

$$\lambda > \frac{hc}{E_G} \tag{1.4.12}$$

In this case, there are no conduction electrons available any longer and the responsivity becomes zero:

$$R_I = \begin{cases} \dfrac{\eta e}{hc}\lambda & \text{for } \lambda \le \lambda_C = \dfrac{hc}{E_G} \\ 0 & \text{for } \lambda > \lambda_C = \dfrac{hc}{E_G} \end{cases} \tag{1.4.13}$$

where λ_C is the cut-off wavelength.

Figure 1.4.2a shows a schematic representation of the current responsivity curve of quantum sensors. In principle, this allows the following conclusions:

- The responsivity of photon sensors is, in principle, wavelength-dependent.
- Photon detectors have a restricted operating wavelength range that is mainly determined by the band structure or band gap E_G. For silicon with $E_G = 1.1$ eV, the cut-off wavelength is

$$\lambda_C = \frac{hc}{E_G} = \frac{6.626 \times 10^{34}\ \mathrm{W\,s^2} \cdot 2.998 \times 10^8\ \mathrm{m/s}}{1.12\ \mathrm{eV}} = 1.11\ \mu\mathrm{m}$$

This is the reason why silicon can only be used for detectors in the near-IR range, whereas the MIR- and FIR-range also can apply other semiconductors.

Table 1.4.1 summarises the differences of the characteristics of thermal and photon sensors.

Table 1.4.1 Comparison of central characteristics of thermal and photon sensors

Parameter	Thermal sensors	Photon sensors
Responsivity	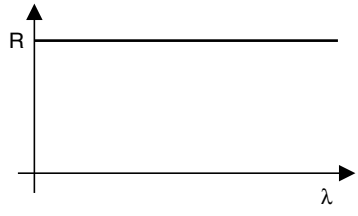	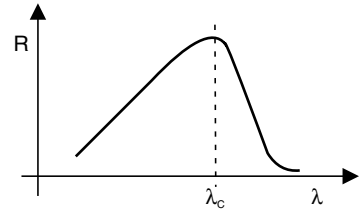
Detectivity D^*	• Wavelength-dependence only. determined by radiation absorption • Wavelength-independent. • Temperature-dependence as power of the temperature. • Only marginal improvement of D^* by cooling.	• Wavelength proportional to λ up to cut-off wavelength λ_C. • Heavily wavelength-dependent (Figure 1.4.1). • Very large D^* values are achievable in the NIR range. • Mostly exponential temperature dependency. • Cooling can largely increase D^*.
Operation	Uncooled	Cooled
Frequency range	Up to several 100 Hz	Up to GHz (photo diodes, photo cells)

Example 1.1: Responsivity and Detectivity of Thermal Sensors and Photon Sensors

The resolution limit of an infrared sensor is absolutely determined by the noise of the detected radiation, that is of the signal to be measured. For thermal sensors it is the radiation noise (Section 4.2.4) and for photon sensors the photon noise. The resulting maximum detectivity is called background-limited infrared photodetection (BLIP) and for thermal sensors background-limited infrared performance. BLIP detectivity for thermal sensors will be presented in Section 5.3. It amounts to:

$$D^*_{\mathrm{BLIP,TH}} = \frac{1}{\sqrt{16\varepsilon k_{\mathrm{B}} \sigma T_{\mathrm{S}}^5}} \tag{1.4.14}$$

with emissivity ε, BOLTZMANN constant k_{B}, STEFAN–BOLTZMANN constant σ as well as sensor temperature T_{S}. The result for $T_{\mathrm{S}} = 300\,\mathrm{K}$ is, according to Example 5.7, a wavelength-independent BLIP detectivity of $D^*_{\mathrm{BLIP,TH}} = 1.81 \times 10^8\,\mathrm{m \cdot Hz^{\frac{1}{2}}\,W^{-1}}$.

For photo sensors, it applies that [1]:

$$D^*_{\mathrm{BLIP,PH}} = \frac{\lambda}{hc}\sqrt{\frac{\eta}{2Q_{\mathrm{B}}}} \tag{1.4.15}$$

with quantum efficiency η, wavelength λ and integral photon exitance of background Q_{B}:

$$Q_{\mathrm{B}} = \sin^2 \frac{\mathrm{FOV}}{2} \int_0^{\lambda_C} Q_{\lambda \mathrm{S}} \, \mathrm{d}\lambda \tag{1.4.16}$$

Here, *FOV* is the field of view (see Section 5.5, Figure 5.5.1). Analogously to spectral exitance $M_{\lambda \mathrm{S}}$ of a blackbody thermal emitter (see Equation 2.3.3), it applies to the spectral photon exitance that

$$Q_{\lambda \mathrm{S}} = \frac{c_1'}{\lambda^4} \frac{1}{e^{\frac{c_2}{\lambda T_{\mathrm{B}}}} - 1} \tag{1.4.17}$$

with radiation constants c_1' and c_2 and background temperature T_{B}.

In the near infrared range, the BLIP detectivity of photon sensors is – by several orders of magnitudes – larger than the detectivity of thermal sensors. In far infrared, that is in the range of maximum radiation of bodies in the ambient temperature range, both have approximately the same magnitude (Figure 1.4.3).

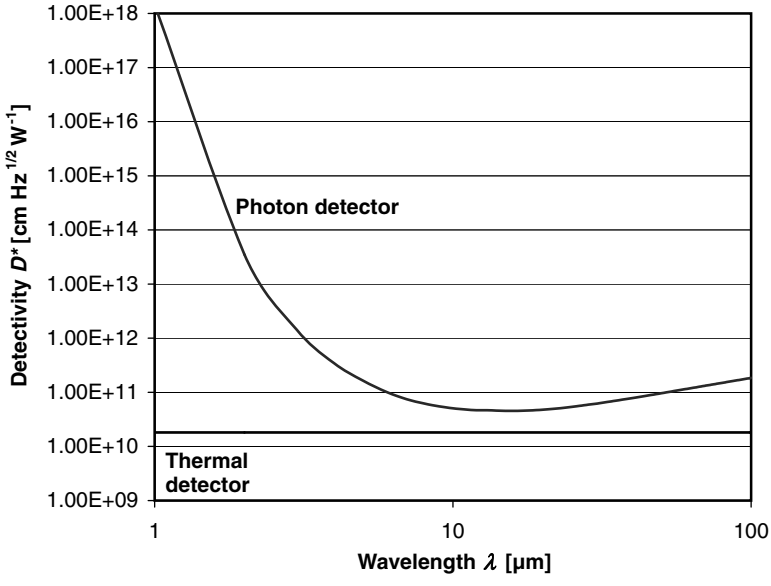

Figure 1.4.3 BLIP detectivity of thermal and photon sensors $FOV = 180°$; $\eta = \varepsilon = 1$; $T_{\mathrm{B}} = T_{\mathrm{S}} = 300\,\mathrm{K}$

1.5 Temperature and Spatial Resolution of Infrared Sensors

The structure of infrared sensors and measuring systems presented in Table 1.1.1 shows that the radiation energy of a measuring object or a radiation source – affected by the transmission

characteristics of the propagation path – can be mapped onto a single-element sensor or an array sensor (FPA). The following practical questions are important:

1. What is the minimum temperature difference of radiation source or measuring object against the background of a single sensor element, and
2. What is the minimum spatial distance between two points with a certain temperature difference that can still be detected by the array sensor.

The temperature resolution is determined by the noise-equivalent temperature difference (*NETD*; see Section 5.4). This is the object's internal temperature difference for which, in the sensor, the noise signal is equivalent to the measuring signal (signal-to-noise ratio $SNR = 1$). *NETD* applies to each individual pixel (sensor element) of a sensor array. The smaller the solid angle that is projected by the imaging system to one sensor pixel, the smaller the sensor signal and thus also *NETD*. Smaller IR measuring systems with a smaller imaging system usually result in a lower-quality temperature resolution.

The modulation transfer function (*MTF*; see Section 5.6) describes the smallest presentable structure and is therefore a measure of the spatial resolution. In principle the spatial resolution is also affected by thermal and electric couplings between the pixels of a sensor array. Optical diffractions and the ratio between pixel dimension and structural size to be imagined have a particularly large influence, though. Especially regarding the latter it becomes obvious very soon that pixels are not able to distinguish the points of the source any longer if the pixel size is larger than half the spatial period of the points.

In principle, a better spatial resolution can be only achieved by smaller pixels. However, this results in a lower-quality temperature resolution, as described above.

Temperature and spatial resolution are two completely different characteristics of sensor arrays. An optimisation of both characteristics partially requires changes of design parameters that are opposed to each other, as the example of the pixel size shows.

1.6 Single-Element Sensors Versus Array Sensors

Section 5.1 to 5.5 present the derivation of sensor parmeters for individual sensor elements that can work both as a separate single-element sensor and an individual pixel of a matrix array sensor (focal plane array, FPA). Section 5.6 will then discuss – separately for array sensors – the spatial resolution of IR sensors, which is only relevant for multi-element sensors.

As Figure 1.6.1 shows that for the signalling chain of a system for contactless temperature measurement, it is theoretically possible to treat sensors with a single sensor surface (single-element sensors) and sensors with many individual sensor surfaces (multi-element sensors, array sensors) exactly in the same way regarding thermal resolution. Each pixel of a thermal imager measures the temperature of a small area of the object and constitutes itself a pyrometer. However, there are different boundary conditions for sensors in pyrometers and in thermal imaging devices. An essential difference is the available sensor surface (field of view). It is practically determined by the optics. For pyrometers, it may amount up to several square millimetres. For pyrometers, the field of view equals the sensor surface. Thermal imaging devices commonly have fields of view with a diagonal of up to 20 mm. In imaging systems, mainly optical distorsion and vignetting restrict the field of view. Only a small

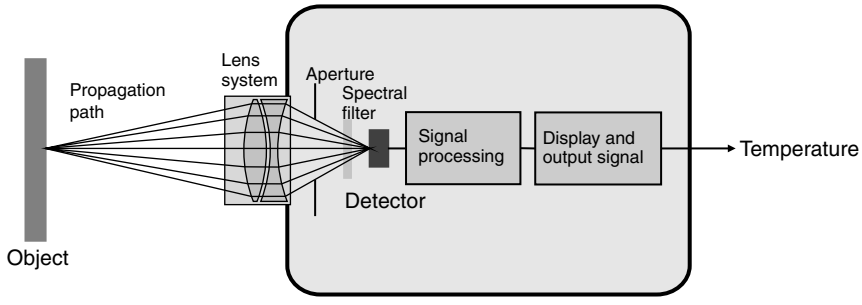

Figure 1.6.1 Signalling chain of a system for contactless temperature measuring

portion of it is available to a pixel of the sensor. With an increasing field of view, also the optical devices and sensors have to be designed larger – which results in a rather substantial increase of the system's total costs. For this reason, the sensor surface should be kept as small as possible. From the sensor's perspective it should be as large as possible, though (Equation 5.4.7).

All the presented types of thermal sensors can be manufactured both as single elements or as array sensors. Examples will, however, only include typical arrangements, such as pyroelectric dual sensors or microbolometer arrays. The micro-bridge technology, for instance, which is presented in the section on microbolometer arrays, is also available for pyroelectric and thermoelectric sensors.

References

1. Caniou, J. (1999) *Passive Infrared Detection, Theory and Application*, Kluwer Academic Publishers, Dordrecht.
2. Herrmann, K. and Walther, L. (1990) *Wissensspeicher Infrarottechnik (Store of Knowledge in Infrared Technology)*, Fachbuchverlag, Leipzig.